ADVANCING EARTH AND SPACE SCIENCES

JGR Solid Earth

RESEARCH ARTICLE
10.1029/2023JB028563

Revisiting the Tianwen Yellow Pumice (TYP) Eruption of Changbaishan Volcano: Tephra Correlation, Eruption Timing and Its Climatostratigraphical Context

Xuan-Yu Chen[1,2], **Yi-Gang Xu**[1,2], **Pavel E. Tarasov**[3], **Christian Leipe**[3,4,5], **Ji-Hoon Kim**[6], **Shuang Yan**[7], **Myong-Ho Park**[8], **Jong-Hwa Chun**[6], **Cong Chen**[9], **Peng-Li He**[1], and **Simon P. E. Blockley**[10]

[1]State Key Laboratory of Isotope Geochemistry, Guangzhou Institute of Geochemistry, Chinese Academy of Sciences, Guangzhou, China, [2]Southern Marine Science and Engineering Guangdong Laboratory (Guangzhou), Guangzhou, China, [3]Paleontology Section, Institute of Geological Sciences, Freie Universität Berlin, Berlin, Germany, [4]Department of Archaeology, Max Planck Institute of Geoanthropology, Jena, Germany, [5]Domestication and Anthropogenic Evolution Independent Research Group, Max Planck Institute of Geoanthropology, Jena, Germany, [6]Marine Geology and Energy Division, Korea Institute of Geoscience and Mineral Resources, Daejeon, South Korea, [7]CAS Key Laboratory of Mineralogy and Metallogeny, Guangzhou Institute of Geochemistry, Chinese Academy of Sciences, Guangzhou, China, [8]CCS Research Center, Kongju National University, Gongju, South Korea, [9]School of Earth Sciences and Engineering, Sun Yat-sen University Zhuhai Campus, Zhuhai, China, [10]Department of Geography, Royal Holloway University of London, Surrey, UK

Abstract Changbaishan volcano (China/North Korea) is one of the most active and hazardous volcanic centers in Northeast Asia. Despite decades of intensive research, the eruption history of this stratovolcano remains poorly constrained. One of the major puzzles is the timing of the eruption that produced the Tianwen Yellow Pumice (TYP) deposit at the caldera rim. Here we identify a new cryptotephra layer in sediment core 13PT-P4 from the East Sea. Grain-specific major, minor, and trace element analyses of glass shards allow a clear correlation of this distal tephra to the proximal TYP deposit of Changbaishan. Age-depth modeling using radiocarbon (^{14}C) dates of sediment bulk organic fractions and other tephrochronological markers from the sediment sequence constraints the age of the cryptotephra and thus the TYP eruption to 29,948–29,625 cal yr BP (95.4% confidence interval). Our findings lead to a revision of the history of Changbaishan explosive activity, and show that the volcano has been particularly active during ca. 51–24 ka BP in the last 100 ka. Using high resolution palaeo-proxy records, we find the TYP tephra almost coeval with regional to hemispheric-scale climatic changes known as Heinrich Event 3 (H3). With its precise age determination and wide geographic dispersion, the tephra offers a key isochron for dating records of past climatic changes and addressing the phasing relationships in environmental response to H3 across East Asia.

Plain Language Summary Improving the knowledge of past volcanism is critical for volcanic hazard mitigation. Changbaishan volcano is one of the most dangerous volcanic centers in Northeast Asia, but its eruption history is not clearly understood. A classic example is the eruption that produced the magnificent Tianwen Yellow Pumice (TYP) deposited at the crater rim. Previous studies suggested a range of very different ages for this major eruption. In this study we trace its volcanic ash into a marine sediment core from the East Sea. By radiocarbon age-depth modeling we are able to say with a high level of certainty that the eruption occurred sometime between 29,948 and 29,625 cal yr BP. The new results demonstrate the dispersal potential of ash from the eruption and shed light on the history and frequency of Changbaishan explosive activity. In addition, the TYP eruption is found to coincide with hemispheric-scale and regional environmental changes. As a consequence, the volcanic ash can be used as a key time mark for dating sediment sequences and for investigating past environmental changes in East Asia. Our study also demonstrates the potential of using distal volcanic ash in reconstructing past explosive volcanism.

1. Introduction

Large volcanic eruptions have substantial influences on the Earth's climate, causing surface cooling and changes in hydrological cycle (Robock, 2000). In addition, these catastrophic events also pose a great threat to modern society and humanity by rapidly releasing huge amounts of energy and pyroclastic materials (e.g., Guffanti

Key Points:

- Timing of the Changbaishan Tianwen Yellow Pumice (TYP) eruption is resolved through proximal-distal tephra correlation and radiocarbon age-depth modeling
- Eruption history of the Changbaishan volcano is revised, and dispersal potential of the TYP tephra is shown for the first time
- A demonstration that the TYP tephra, as a regional marker, has great potential for sediment sequence-based palaeoenvironmental studies

Supporting Information:

Supporting Information may be found in the online version of this article.

Correspondence to:

X.-Y. Chen,
xuanyuchen@gig.ac.cn

Citation:

Chen, X.-Y., Xu, Y.-G., Tarasov, P. E., Leipe, C., Kim, J.-H., Yan, S., et al. (2024). Revisiting the Tianwen Yellow Pumice (TYP) eruption of Changbaishan volcano: Tephra correlation, eruption timing and its climatostratigraphical context. *Journal of Geophysical Research: Solid Earth*, *129*, e2023JB028563. https://doi.org/10.1029/2023JB028563

Received 17 DEC 2023
Accepted 9 APR 2024

Author Contributions:

Conceptualization: Xuan-Yu Chen, Yi-Gang Xu, Pavel E. Tarasov, Simon P. E. Blockley
Data curation: Xuan-Yu Chen, Shuang Yan, Cong Chen, Peng-Li He
Formal analysis: Xuan-Yu Chen
Funding acquisition: Xuan-Yu Chen, Yi-Gang Xu
Investigation: Xuan-Yu Chen, Pavel E. Tarasov
Methodology: Xuan-Yu Chen, Shuang Yan, Peng-Li He
Project administration: Yi-Gang Xu

Resources: Ji-Hoon Kim, Myong-Ho Park, Jong-Hwa Chun
Supervision: Yi-Gang Xu, Simon P. E. Blockley
Validation: Xuan-Yu Chen, Christian Leipe
Visualization: Xuan-Yu Chen
Writing – original draft: Xuan-Yu Chen
Writing – review & editing: Yi-Gang Xu, Pavel E. Tarasov, Christian Leipe, Ji-Hoon Kim, Shuang Yan, Myong-Ho Park, Jong-Hwa Chun, Cong Chen, Simon P. E. Blockley

et al., 2009). Yet our understanding of these eruptions is not comprehensive. Changbaishan (also known as Baegdusan) volcano, located on the border between China and North Korea (Figure 1a), is the largest and most active intraplate volcanic center in NE Asia (Wei et al., 2013; Zhang et al., 2018). The volcano is well known for its Millennium Eruption (ME) in 946 CE (Oppenheimer et al., 2017; Sigl et al., 2015; Xu et al., 2013), with a Volcanic Explosivity Index (VEI) of 6–7 (Horn & Schmincke, 2000; Newhall et al., 2018; Q. Yang et al., 2021) and sulfur emission exceeding that of the 1815 CE eruption of Tambora (Iacovino et al., 2016). With the exception of the ME, other eruptions of the volcano remain poorly constrained since the proximal stratigraphies are in general, not well exposed or largely inaccessible. The unknown characteristics of those less studied eruptions include their timing, magnitude, tephra distribution, and potential environmental effects.

In recent years, Changbaishan has experienced increased seismic, geodetic, and geothermal anomalies (Xu et al., 2012), which raise concerns about its potential volcanic hazard. Improving the chronology of past volcanism is important for hazard risk assessment, by providing critical information on the volcano's past eruptive behavior, patterns and potential. However, dating young eruptions (<100 ka) of Changbaishan has proven very challenging in the few accessible proximal outcrops (e.g., Ramos et al., 2016). A classic example is the yellow to gray colored pumice deposit at the Tianwen Summit of the caldera rim (hereby named Tianwen Yellow Pumice (TYP), Figure 1b). This ca. 50 m thick lapilli fall deposit is over 30 times thicker than the overlying ME fall units (ca. 1.5 m, Figure 1b) that have been distally transported over 9,000 km to Greenland (Sun et al., 2014). Given its huge thickness, much attention has been drawn to the TYP deposit, especially to the timing and nature of the associated eruption. Nevertheless, the age of the TYP eruption is still under debate despite decades of studies involving multiple dating methods. For example, luminescence techniques yield ages for the TYP eruption ranging from 1.3 (±0.2) to 2.0 (±0.7) ka (Ji et al., 1999; Sun et al., 2017), whereas Ar-Ar (L. Yang et al., 2014) and U-series (F. Wang et al., 2001) methods date the eruption to 4.2 (±0.4) and 5.3 (±2.4) ka, respectively (Figure 1c). An earlier study employing radiocarbon (^{14}C) dating suggests an age of ca. 4.1 ka BP (Liu et al., 1998). In contrast, tephrochronology suggests a Pleistocene age (ca. 50.6 ka, Pan et al., 2020) via a correlation based on major element geochemistry of the TYP to a distal Changbaishan tephra (Baegdusan-Japan (B-J), Lim et al., 2013). All these chronological discordances have long prevented a sound understanding of the TYP eruption and the wider history of Changbaishan's volcanic activities, which complicates the evaluation of the risk of future eruptions.

The contradictions mentioned above can be resolved by reliably identifying the eruptive products in distal realms, using both major and trace element glass compositions of tephra. This approach offers a much more secure level of geochemical correlation of tephra layers compared to using major elements alone (e.g., Tomlinson et al., 2012, 2015). In principle, if robust proximal–distal tephra correlations can be established, the chronological information of a given eruption can be evaluated (Lowe, 2011). In this study, we investigate a sediment core collected from the East Sea (also known as the Sea of Japan) using the cryptotephra extraction techniques (Blockley et al., 2005), aiming to trace the tephra of the TYP eruption into the marine record and to date the eruption using age-depth model of the marine sequence. With these new findings, we attempt to clarify the Changbaishan eruption history, and to evaluate the potential of the distal TYP tephra as a key marker and isochron for palaeoenvironmental studies.

2. Materials and Cryptotephra Extraction Methods

2.1. East Sea Marine Core 13PT-P4 and Cryptotephra Extraction

The East Sea is characterized as a semi-enclosed marginal sea, encircled by the Asian mainland, the Japanese Islands, and Sakhalin in the northwestern sector of the Pacific Ocean (Figure 1a). The piston core 13PT-P4 (37° 00′52″ N, 130°15′58″E) possesses an overall length of 764 cm and was obtained at a water depth of 2,164 m from the southwestern part of the sea (Figure 1a). The core predominantly comprises hemipelagic muds and turbidites, featuring intercalated lapilli and ash layers within the sediments (Chen et al., 2022). These characteristics are commonly observed in sediment cores retrieved from the same region (e.g., Chun et al., 1997; Park et al., 2003). A pronounced lapilli layer at 173–174 cm core depth has been identified and correlated to the Ulleung-Oki (U-Oki) tephra (ca. 10.2 ka, Smith et al., 2011) from Ulleungdo volcano, South Korea (Chen et al., 2022). The study also reveals a number of Holocene cryptotephra layers preserved in the core above the U-Oki tephra (Chen et al., 2022), which were previously unknown based on visible tephra inspection. Further cryptotephra investigation has therefore been undertaken for the late Pleistocene core section below the U-Oki tephra.

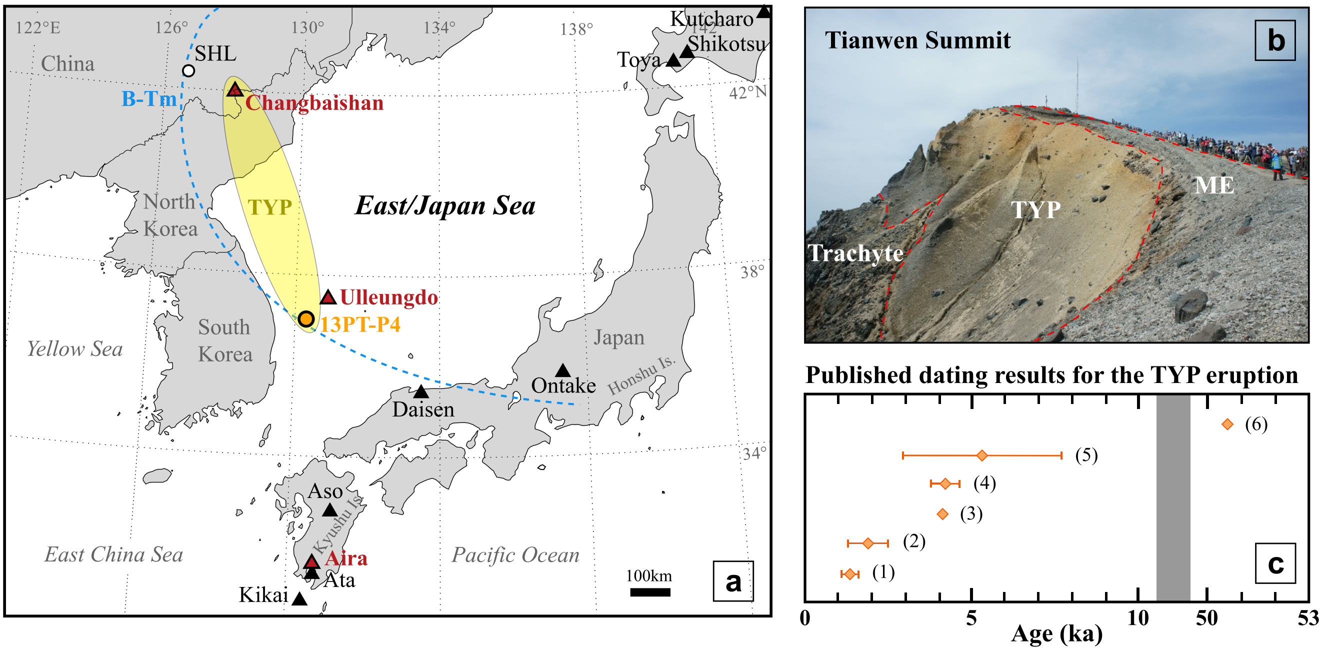

Figure 1. (a) Map of the East Asia showing locations of Changbaishan, Ulleungdo, and Aira volcanoes, marine core 13PT-P4, Lake Sihailongwan (SHL), and other major volcanic centers in and around the East Sea which have produced regional tephra markers spanning the last 100 ka. A yellow ellipse indicates dispersion of tephra from the Changbaishan Tianwen Yellow Pumice (TYP) eruption shown by this study. Distribution of the B-Tm (Baegdusan-Tomakomai) tephra from the Changbaishan Millennium Eruption (ME) is also shown (dashed blue line; data sources: Chen et al., 2016, 2022; McLean et al., 2016; Sun et al., 2015). (b) Photo showing the TYP deposit and the ME fall units at the Tianwen Summit on the caldera rim of Changbaishan. (c) Published dating results (±2*σ*) for the TYP eruption (references include: Ji et al., 1999; Liu et al., 1998; Pan et al., 2020; Sun et al., 2017; F. Wang et al., 2001; L. Yang et al., 2014).

In this study, we reported on a cryptotephra identified in-between two visible tephra layers in the core section spanning 380–440 cm (Figure 2). Cryptotephra extraction followed the methods outlined by Blockley et al. (2005). The sediment underwent initial continuous sub-sampling at a 5 cm resolution (referred to as a "range-finder" sample) to ascertain the presence of tephra. In cases where an elevated peak in glass shard concentration was identified in a range-finder sample, the sediment was subsequently re-sampled at a 1 cm resolution (referred to as a "point sample") to pinpoint the exact stratigraphic position of the peak. All samples underwent wet sieving through meshes of 125 and 15 μm, and the residues between these two grain sizes were subsequently treated using the stepwise heavy liquid flotation method (Blockley et al., 2005). Blank samples were concurrently prepared with all specimens to oversee potential laboratory contamination. Extracted samples were affixed to slides with Canada Balsam, and the enumeration of glass shards was performed using a polarized light microscope to ascertain the quantity of shards per gram of dried sediment (shards/g). *Lycopodium* spores (Stockmarr, 1971) were used to estimate the tephra shard concentration, given the large numbers of shards presented in the sediment. Glass shards from the point sample displaying peak tephra concentration were extracted again from the sediment and affixed using Epoxy resin. The mounted shards were subsequently sectioned and polished for the purpose of geochemical analysis.

2.2. Tianwen Yellow Pumice

The investigated proximal Tianwen Summit section (Figure 1b; 42°01′33″ N, 128°04′00″E) is located on the northern rim of the caldera. At this outcrop, the ca. 50 m thick gray to yellow TYP pyroclastic fall unit is under tight stratigraphic control, which overlies the cone building trachyte and underlies the fall deposits produced by the ME (Figure 1b; also see Chen et al. (2016)). Lapilli-sized samples were collected from the TYP fall unit, which were crushed, cleaned and dried in the laboratory. Clean fragments were selected through microscopic examination and mounted using Epoxy resin. The samples were sectioned and polished before geochemical analysis.

10.1029/2023JB028563

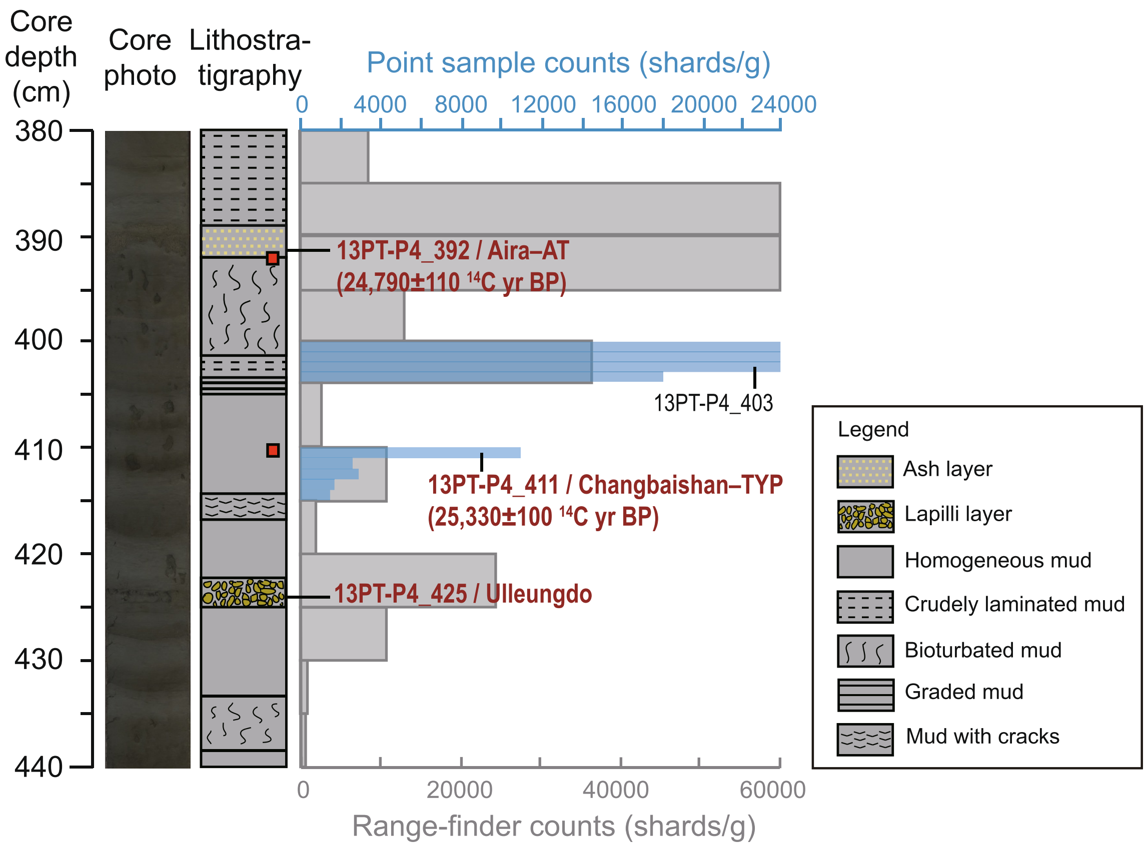

Figure 2. Core photo, lithostratigraphy and glass shard concentrations profile for the reported section of core 13PT-P4 (see Figure 1a for location). Range-finder and point sample shard counts are capped at 60,000 and 24,000 shards/g, respectively. Tephra layers are coded using the name of the core and their composite depths, with horizons related to this study highlighted in red. The proposed correlations for the reported tephra layers are shown as source volcano–eruption event. Red squares indicate where sediment samples were taken for ^{14}C dating, and the results are shown as $\delta^{13}C$ corrected conventional ^{14}C date.

3. Geochemical and Radiometric Analytical Methods

3.1. Wavelength-Dispersive Electron Probe Microanalysis (WDS-EPMA)

Major and minor element glass compositions of the reported tephra layers were measured using WDS-EPMA at the State Key Laboratory of Isotope Geochemistry at Guangzhou Institute of Geochemistry Chinese Academy of Sciences with a Cameca SXFiveFE, and at the Tephra Analysis Unit at the University of Edinburgh (UK) with a Cameca SX100. Operating conditions of the two instruments were exactly the same, with a beam size of 5 μm, an accelerating voltage of 15 kV, a beam current of 2 nA for Na, Al, Si, K, Ca, Mg, and Fe, and a bean current of 80 nA for P, Ti, and Mn, following the 5 μm set-up in Hayward (2011). Before, after and in-between analytical sessions, secondary glass standards were analyzed to evaluate both instrumental accuracy and analytical precision. The data underwent filtration to eliminate non-glass analyses and those with analytical totals <95%. To facilitate comparison, all data presented in this paper were normalized to 100 wt.% on a volatile-free basis. The raw data and glass standards are available in Supporting Information S1.

3.2. Laser Ablation Inductively Coupled Plasma Mass Spectrometry (LA-ICP-MS)

Trace element glass compositions of the proximal and distal Changbaishan tephras were measured using LA-ICP-MS at the CAS Key Laboratory of Mineralogy and Metallogeny, Guangzhou Institute of Geochemistry Chinese Academy of Sciences. The system consists of a Thermo Fisher Scientific iCAP RQ ICP-MS, coupled to an Applied Spectra Inc. J200 Tandem QX 343 nm femtosecond laser ablation system. A spot size of 20 μm was used for all analyses. Operating conditions of the instrument were as follows: a repetition rate of 6 Hz with 60% energy, a 20 s count time on the sample and 20 s on the gas blank (background). The analysis of reference glass standards (ATHO-G, StHs6/80-G, and NIST612; Jochum et al., 2006) was conducted before, after and between sessions to monitor both instrumental accuracy and analytical precision. Concentrations were calibrated using NIST612 with ^{29}Si as the internal standard. The off-line selection, integration of the background and analytical signals, time-drift correction and quantitative calibration were performed using the Iolite software (Paton et al., 2011). Accuracies of the ATHO-G glass analyses are typically <5% for most elements, and <10% for Nb and Ta. Reproducibility of ATHO-G analyses is <5% RSD for all trace elements. Full trace element data sets and secondary standard analyses are provided in Supporting Information S1.

3.3. Radiocarbon (^{14}C) Dating

Sediment samples associated with the reported visible and cryptotephra layers of the 13PT-P4 core were dated using the ^{14}C method. The total organic carbon (TOC) fraction of sediment was utilized for accelerator mass spectrometry ^{14}C dating at Beta Analytic Testing Laboratory, Florida, USA. The sediments underwent pretreatment employing the acid wash method (Beta Analytic Testing Laboratory: https://www.radiocarbon.com/carbon-dating-pretreatment.htm) to remove secondary carbon components that might lead to erroneous results. The final results were reported as $\delta^{13}C$ corrected conventional ^{14}C ages in Table 1, and the relevant marine reservoir correction and calibration are discussed in Section 4.

4. Results and Tephra Provenance

4.1. Tephrostratigraphy, ^{14}C Chronology and Glass Geochemistry of 13PT-P4 Tephra Layers

Two visible tephra layers (13PT-P4_392 and 13PT-P4_425) and two cryptotephra horizons (13PT-P4_403 and 13PT-P4_411) are identified within the reported core section (380–440 cm, Figure 2). Of relevance to this study are the cryptotephra 13PT-P4_411 and the two visible tephra layers 13PT-P4_392 and 13PT-P4_425 (Table 1).

Identified at the core depth of 392–389 cm, 13PT-P4_392 is a visible layer containing light gray colored coarse-grained (2–1/16 mm) ash (Figure 2). Glass shards from this layer are dominantly colorless platy and featureless shards. Geochemically, glass shards of the layer are relatively homogenous and highly evolved (SiO_2: 77.2–78.6 wt.%, Table 1), and have comparatively low alkaline ($Na_2O + K_2O$: 6.4–7.3 wt.%), FeO_t (1.0–1.4 wt.%) and TiO_2 (0.1–0.2 wt.%) contents (Table 2). ^{14}C dating on the TOC fraction of the associated sediment sample suggests a conventional ^{14}C date of 24,790 ± 110 ^{14}C yr BP for this tephra (Figure 2, Table 1).

13PT-P4_411 is a cryptotephra layer identified at the core depth of 411–410 cm (Figure 2), with tephra concentration of ca. 10,800 shards/g. This layer has a clearly defined stratigraphic position (Figure 2), and comprises glass shards characterized by fluted, cuspate and vesicular features. Glass shards from this layer are compositionally heterogeneous (SiO_2: 69.7–74.1 wt.%), displaying moderate alkaline ($Na_2O + K_2O$: 9.2–10.8 wt.%) and TiO_2 (0.3–0.4 wt.%), low CaO (0.3–0.7 wt.%), and significantly elevated FeO_t (5.0–5.7 wt.%) contents (Table 2). Consistent with the major element compositions, the incompatible trace element concentrations of the 13PT-P4_411 glasses are also heterogeneous (85–150 ppm Y, 1,359–2,703 ppm Zr, and 26–54 ppm Th; Table 2). ^{14}C dating of the associated sediments suggests a conventional age of 25,330 ± 100 ^{14}C yr BP for the cryptotephra (Figure 2, Table 1).

A 3 cm-thick lapilli layer is identified at the core depth of 425–422 cm and designated as 13PT-P4_425 (Figure 2). This layer consists of lapilli-sized pumices with diameter ranging from 2 to 5 mm. Glass compositions of pumices from the layer are very homogeneous and have the lowest silica contents (SiO_2: 60.2–61.0 wt.%) among all the reported marine tephras. Glasses of the layer are characterized by significantly elevated alkaline ($Na_2O + K_2O$: 13.5–14.2 wt.%), relatively high Al_2O_3 (18.7–19.3 wt.%) and TiO_2 (ca. 0.6 wt.%), and intermediate FeO_t (3.4–3.8 wt.%) contents (Table 2). Although the 13PT-P4_425 is located only 11 cm below the cryptotephra 13PT-P4_411 (Figure 2), geochemical analysis reveals distinct glass compositions for the two tephra layers (Table 2), eliminating the possibility of the cryptotephra being reworked from the underlying visible layer.

4.2. Glass Geochemistry of Changbaishan TYP Deposit

Major and minor element glass compositions of the Changbaishan proximal TYP deposit have previously been reported in Chen et al. (2019) coded as the C-4 unit. The TYP glasses have heterogeneous compositions (SiO_2: 69.8–73.5 wt.%), with moderate alkaline ($Na_2O + K_2O$: 8.8–10.9 wt.%), low CaO (0.3–0.6 wt.%), and elevated FeO_t (4.8–5.6 wt.%) contents (Table 2). As with the major element compositions, the trace element analysis

10.1029/2023JB028563

Table 1
Summary Table of Tephrostratigraphic, Geochemical, Chronological, and Provenance Information for the Reported Distal Tephra Layers From the 13PT-P4 Core

Tephra label	Core segment	Core depth (cm)	Form of preservation	Glass shard concentration (shards/g)	Glass shard morphology	Major element glass compositions of dominant population (wt.%)				^{14}C lab code	Dated material	$\delta^{13}C$ (‰)	Conventional ^{14}C age (BP)	Tephra correlation
						SiO_2	CaO	K_2O	n					
13PT-P4_392	2a	389–392	Ash layer	>1,000,000	Platy	77.22–78.58	1.06–1.23	3.01–3.54	10	Beta-644957	Bulk sediment (total organic carbon)	−23.3	24,790 ± 110	Aira, AT
13PT-P4_411	2a	410–411	Cryptotephra	10,862	Fluted, cuspate, vesicular	69.70–74.06	0.30–0.71	4.20–4.93	32	Beta-648369	Bulk sediment (total organic carbon)	−22.6	25,330 ± 100	Changbaishan, TYP
13PT-P4_425	2a	422–425	Lapilli layer	24,208	Highly vesicular	60.24–61.02	1.59–1.75	6.78–7.34	10		N/A			Ulleungdo, unknown eruption

Table 2
Summary Table of Major, Minor, and Trace Element Glass Compositions of the Distal 13PT-P4 Tephra Layers and the Proximal Tianwen Yellow Pumice Deposit

Location	East Sea/Sea of Japan						Changbaishan	
Tephra layer/unit	13PT-P4_392		13PT-P4_411		13PT-P4_425		TYP	
Major elements wt.%	Mean	±1σ	Mean	±1σ	Mean	±1σ	Mean	±1σ
SiO_2	77.79	0.42	71.73	1.16	60.71	0.24	71.66	0.83
TiO_2	0.13	0.01	0.36	0.03	0.59	0.03	0.33	0.03
Al_2O_3	12.49	0.20	11.98	0.80	18.99	0.20	11.45	0.57
FeO_t	1.28	0.11	5.32	0.20	3.55	0.13	5.16	0.17
MnO	0.04	0.00	0.12	0.01	0.17	0.01	0.12	0.03
MgO	0.14	0.02	0.02	0.03	0.33	0.04	0.02	0.03
CaO	1.14	0.05	0.50	0.12	1.66	0.06	0.42	0.08
Na_2O	3.70	0.26	5.42	0.34	6.83	0.10	5.53	0.48
K_2O	3.25	0.14	4.54	0.15	7.07	0.15	4.82	0.16
P_2O_5	0.03	0.01	0.02	0.02	0.10	0.02	0.02	0.02
$Na_2O + K_2O$	6.95	0.30	9.96	0.36	13.90	0.21	10.35	0.43
n	10		32		10		36	
Reference	This study		This study		This study		Chen et al. (2019)	

Location	East Sea/Sea of Japan	Changbaishan
Tephra layer/unit	13PT-P4_411	TYP
Trace elements (ppm)	Range	Range
Rb	227.4–365.5	243.3–494.5
Sr	0.5–4.2	0.5–4.2
Y	84.6–149.8	86.9–170.0
Zr	1,358.7–2,703.1	1,551.9–3,318.8
Nb	162.9–307.0	190.7–346.8
Ba	2.9–12.6	2.4–6.9
La	139.3–264.4	147.3–275.1
Ce	274.1–498.9	295.6–507.8
Pr	28.8–92.6	31.5–86.1
Nd	109.8–189.8	111.9–208.1
Sm	22.9–39.4	21.7–40.0
Eu	0.2–0.7	0.3–1.0
Gd	18.5–38.4 (83.9[a])	19.3–35.1
Tb	2.8–5.1	3.0–5.7
Dy	17.1–31.2	17.4–36.0
Ho	3.3–5.9	3.2–6.7
Er	8.7–16.6	8.4–17.8
Tm	1.1–2.1	1.2–2.4
Yb	7.6–13.8	7.9–15.0
Lu	0.9–1.9	1.0–2.2
Hf	32.5–63.5	34.8–77.9
Ta	9.3–17.1	10.2–20.9

10.1029/2023JB028563

Table 2
Continued

Location	East Sea/Sea of Japan	Changbaishan
Tephra layer/unit	13PT-P4_411	TYP
Trace elements (ppm)	Range	Range
Pb	25.6–49.7	27.4–63.8
Th	26.3–53.5	27.9–60.4
U	5.4–11.6	5.5–12.5
n	18	32
Reference	This study	This study

[a]Value in parenthesis is an outlier.

conducted in this study reveals that the TYP glasses are heterogeneous in terms of their incompatible trace element concentrations, with 87–170 ppm Y, 1,552–3,319 ppm Zr, and 28–60 ppm Th (Table 2).

4.3. Provenance and Age of 13PT-P4 Tephra Layers

In order to determine the provenance of the identified marine tephra layers, we establish a database containing the most widespread tephra markers in and around the East Sea spanning the last 100 ka, based on the summaries in Machida and Arai (2003) and Albert et al. (2019). Tephra markers included in the database are from volcanoes in Japan, South Korea and China/North Korea, with a VEI ≥ 6 (Table S1 in Supporting Information S1).

The visible ash layer 13PT-P4_392 has rhyolitic glass compositions (Figure 3a). Comparison of major and minor element glass compositions of this layer with those in the database reveals a match with the Aira-Tanzawa (AT) tephra from Aira Caldera, Japan (Figure 3). In addition, our marine conventional ^{14}C date of the tephra (24,790 ± 110 ^{14}C yr BP) matches closely with the terrestrial conventional ^{14}C dates of the AT tephra (e.g., 24,790 ± 350 ^{14}C yr BP, Ikeda et al., 1995; 24,830 ± 90 ^{14}C yr BP, Smith et al., 2013). Taken together, tephra layer 13PT-P4_392 can be confidently correlated to the AT tephra.

Glasses of the 13PT-P4_411 cryptotephra are also rhyolitic in composition, straddling the boundary between the alkaline and subalkaline series (Figure 3a). Detailed source discrimination using the tephra database reveals that the cryptotephra likely originates from the Changbaishan volcano, given its geochemical affinity to the Changbaishan tephra (Figure 3). In contrast, the underlying 13PT-P4_425 is product of the Ulleungdo volcano, whose tephras are typically phonolitic to trachytic in composition (Figure 3). It is worth noting that the entire pre-Holocene tephra record of the 13PT-P4 core has been geochemically fingerprinted, but only the 13PT-P4_411 shows a geochemical affinity to Changbaishan.

Marine TOC ^{14}C dating suggests a conventional ^{14}C age of 25,330 ± 100 ^{14}C yr BP for the 13PT-P4_411 cryptotephra. In general, any marine-derived conventional ^{14}C date needs to be corrected for the marine reservoir effect (expressed as marine reservoir age R; Stuiver et al., 1986) before being calibrated to a calendar age (Alves et al., 2018), usually a local ΔR variation from the modeled global marine reservoir age R_g of 400 years (Reimer et al., 2009). However, the identical marine and terrestrial conventional ^{14}C dates of the AT/13PT-P4_392 tephra (24,790 ± 110 ^{14}C yr BP) indicates a negligible R, and thus a ΔR for this location and time period of −400 for the dated TOC fraction, essentially requiring no reservoir correction. Assuming this local ΔR holds true for a few hundred years, the marine ^{14}C date for the 13PT-P4_411 tephra (25,330 ± 100 ^{14}C yr BP) is therefore equal to its terrestrial-derived ^{14}C date and can thus be calibrated using the terrestrial IntCal20 curve (Reimer et al., 2020), which yields a calendar age of 29,921–29,255 cal yr BP (95.4%, Figure S1 in Supporting Information S1). Such an approach is supported by the δ^{13}C values of the reported ^{14}C dates (Table 1), which are much closer to values expected for terrestrial and not marine samples (e.g., Li et al., 2017; Muglia et al., 2023), perhaps indicating a significant supply of organic carbon running in from terrestrial sources at this time.

10.1029/2023JB028563

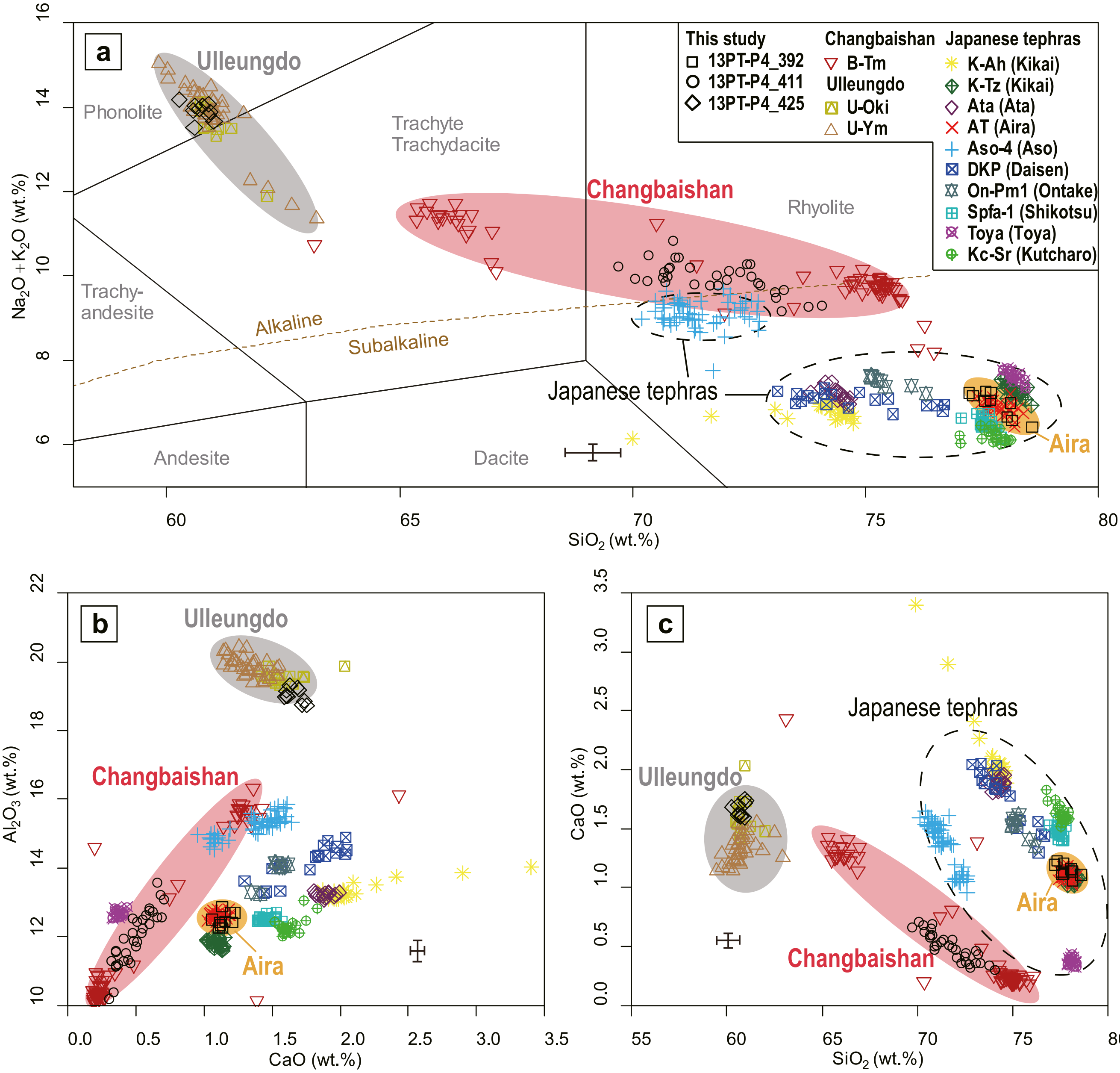

Figure 3. Major and minor element (a) total alkali versus silica diagram (Le Bas et al., 1986) and (b, c) bivariate plots showing glass compositions of the 13PT-P4_392, 13PT-P4_411, and 13PT-P4_425 tephras, along with glass compositions of the most widespread tephra markers in and around the East Sea spanning the last 100 ka for comparison. Detailed information of the tephra markers and their associated eruptions is given in Table S1 in Supporting Information S1. For locations of their source volcanoes see Figure 1a. Reference data sources: Changbaishan volcano, China/North Korea (Chen et al., 2016); Ulleungdo volcano, South Korea (McLean et al., 2020; Smith et al., 2011); Japanese volcanoes (Kikai, Ata, Aira, Aso, Daisen, Ontake, Shikotsu, Toya, and Kutcharo; Albert et al., 2018, 2019; Smith et al., 2013). Error bars represent 2x standard deviation of repeat analyses of the ATHO-G standard glass.

5. Discussion

5.1. Tephra Correlation for Changbaishan TYP Eruption

In order to resolve the timing of the TYP, we attempt to correlate this proximal tephra deposit to its distal counterpart. Previous distal tephra studies have documented eight explosive eruptions from Changbaishan over the last 100 ka, which produced tephra layers of B-Ym (ca. 86 ka, Lim et al., 2013), B-Sado (ca. 70 ka, Derkachev et al., 2019; Lim et al., 2013), B-J (ca. 51 ka, Chun et al., 2006; Lim et al., 2013), B-Sg-42 (ca. 42 ka, McLean et al., 2020), B-Un1 (ca. 38 ka, Derkachev et al., 2019), B-V (ca. 25 ka, Machida & Arai, 2003), B-Sg-08 (ca. 8 ka,

10.1029/2023JB028563

Table 3
Summary Information of the Distal Changbaishan Tephra Records Spanning the Last 100 ka

Research status	Tephra code	Tephra name	Location of identification	Reference for major and minor element glass compositions	Reference for trace element glass compositions	Age	References for age
Previously documented	B-Tm	Baegdusan-Tomakomai	East Sea/Japanese Islands/ Greenland ice-cores[a]	Chen et al. (2016)	Chen et al. (2016)	946 CE	Xu et al. (2013), Sigl et al. (2015), and Oppenheimer et al. (2017)
	B-Sg-08	Baegdusan-Suigetsu-08	Central Japan	McLean et al. (2018)	McLean et al. (2020)	8,166–8,099 cal yr BP (95.4%)	McLean et al. (2018)
	B-V	Baegdusan-Vladivostok	East Sea	Derkachev et al. (2019)	N/A	ca. 24.5 ka/ca. 29.4–29.0 ka	Machida and Arai (2003) and Derkachev et al. (2019)
	B-Un1	Baegdusan-Unknown	East Sea	Derkachev et al. (2019)	N/A	ca. 38.3 ka	Derkachev et al. (2019)
	B-Sg-42	Baegdusan-Suigetsu-42	Central Japan	McLean et al. (2020)	McLean et al. (2020)	42,750–42,323 cal yr BP (95.4%)	McLean et al. (2020)
	B-J	Baegdusan-Japan Basin	East Sea	Ikehara et al. (2004)	N/A	ca. 51–48 ka	Ikehara et al. (2004), Chun et al. (2006), Lim et al. (2013), and Derkachev et al. (2019)
	B-Sado	Baegdusan-Sado	East Sea	Derkachev et al. (2019)	N/A	ca. 67.6 ka/ca. 71.9–71.1 ka	Lim et al. (2013) and Derkachev et al. (2019)
	B-Ym	Baegdusan-Yamato	East Sea	Lim et al. (2013)	N/A	ca. 85.8 ka	Lim et al. (2013)
Newly identified	13PT-P4_411	Tianwen Yellow Pumice	East Sea	This study	This study	29,948–29,625 cal yr BP (95.4%)	This study

[a]References for identification of the B-Tm tephra include Sun et al. (2014, 2015), Chen et al. (2016, 2022), and McLean et al. (2016).

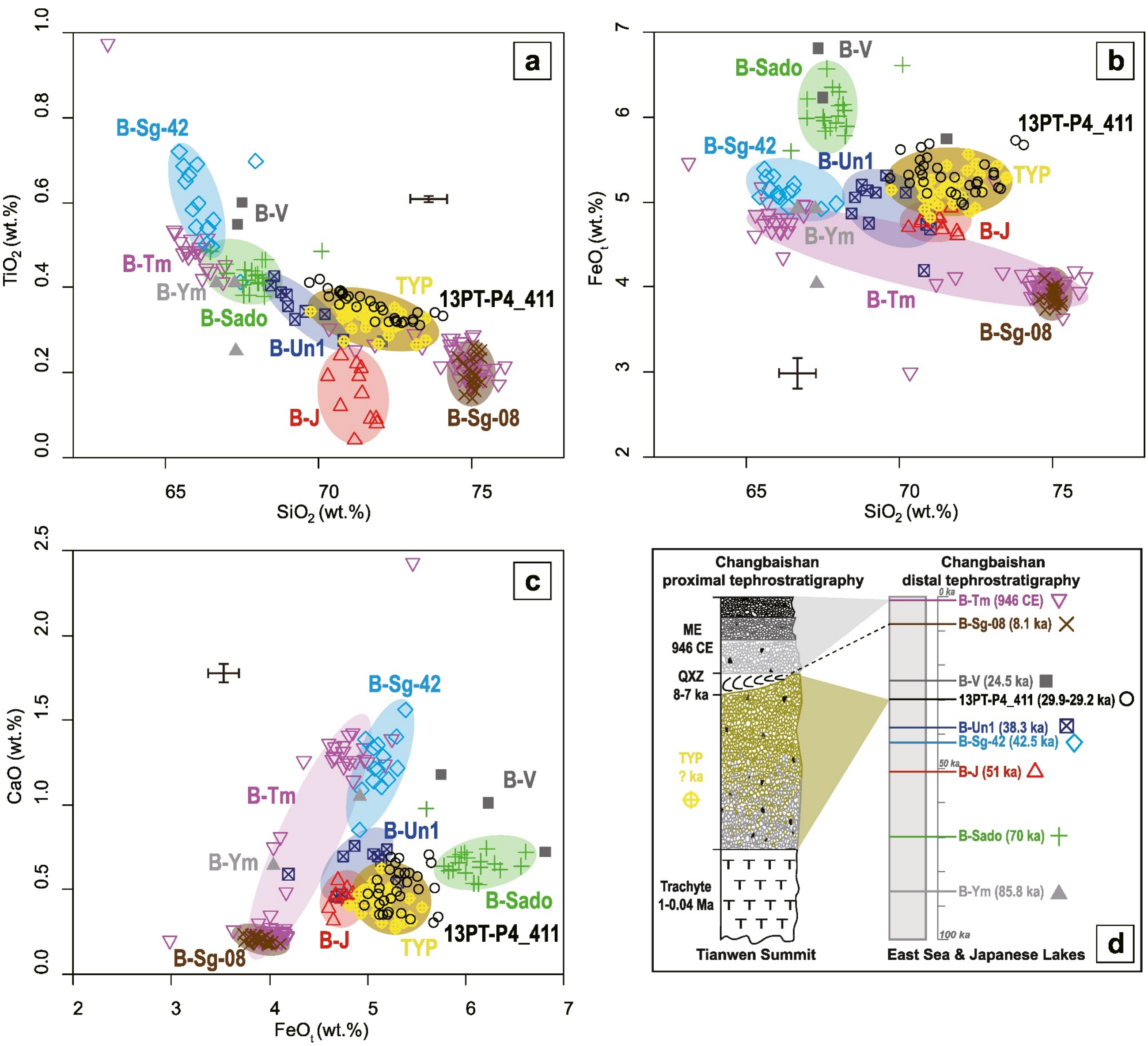

Figure 4. (a–c) Major and minor element bivariate plots showing glass compositions of the proximal Tianwen Yellow Pumice deposit (Chen et al., 2019), distal 13PT-P4_411 tephra (this study), along with other distal Changbaishan tephras spanning the last 100 ka for comparison (for legend see subfigure (d)), and (d) compiled Changbaishan proximal and distal tephrostratigraphies with age of the tephra layers, legend of geochemical analyses, and proximal–distal tephra correlations shown. Detailed information and references of the distal Changbaishan tephras see Table 3. Error bars represent 2x standard deviation of repeat analyses of the ATHO-G standard glass. References for geochemical data of distal Changbaishan tephras: B-Tm (Chen et al., 2016), B-Sg-08 (McLean et al., 2018), B-V (Derkachev et al., 2019), B-Un1 (Derkachev et al., 2019), B-Sg-42 (McLean et al., 2020), B-J (Ikehara et al., 2004), B-Sado (Derkachev et al., 2019), and B-Ym (Lim et al., 2013). References for stratigraphic and chronological data of proximal volcanic stratigraphy: Millennium Eruption (Chen et al., 2016; Oppenheimer et al., 2017; Sigl et al., 2015; Xu et al., 2013), Qixiangzhan (QXZ, Pan et al., 2020, 2022; Sun et al., 2018).

McLean et al., 2018), and B-Tm (946 CE, Chen et al., 2016; McLean et al., 2016; Oppenheimer et al., 2017; Sun et al., 2014) preserved in lacustrine, marine and glacial environments (Table 3). Here, we propose the identification of an additional distal Changbaishan tephra (i.e., 13PT-P4_411) based on its geochemical affinities to the volcano (Figure 3). While showing Changbaishan affinities, this newly discovered tephra has an eruption age (ca. 29.9–29.2 ka) and glass compositions distinguishable from the eight documented distal Changbaishan tephras (Figure 4), meaning that it represents a previously unknown Changbaishan eruption that was capable of dispersing ash to the East Sea.

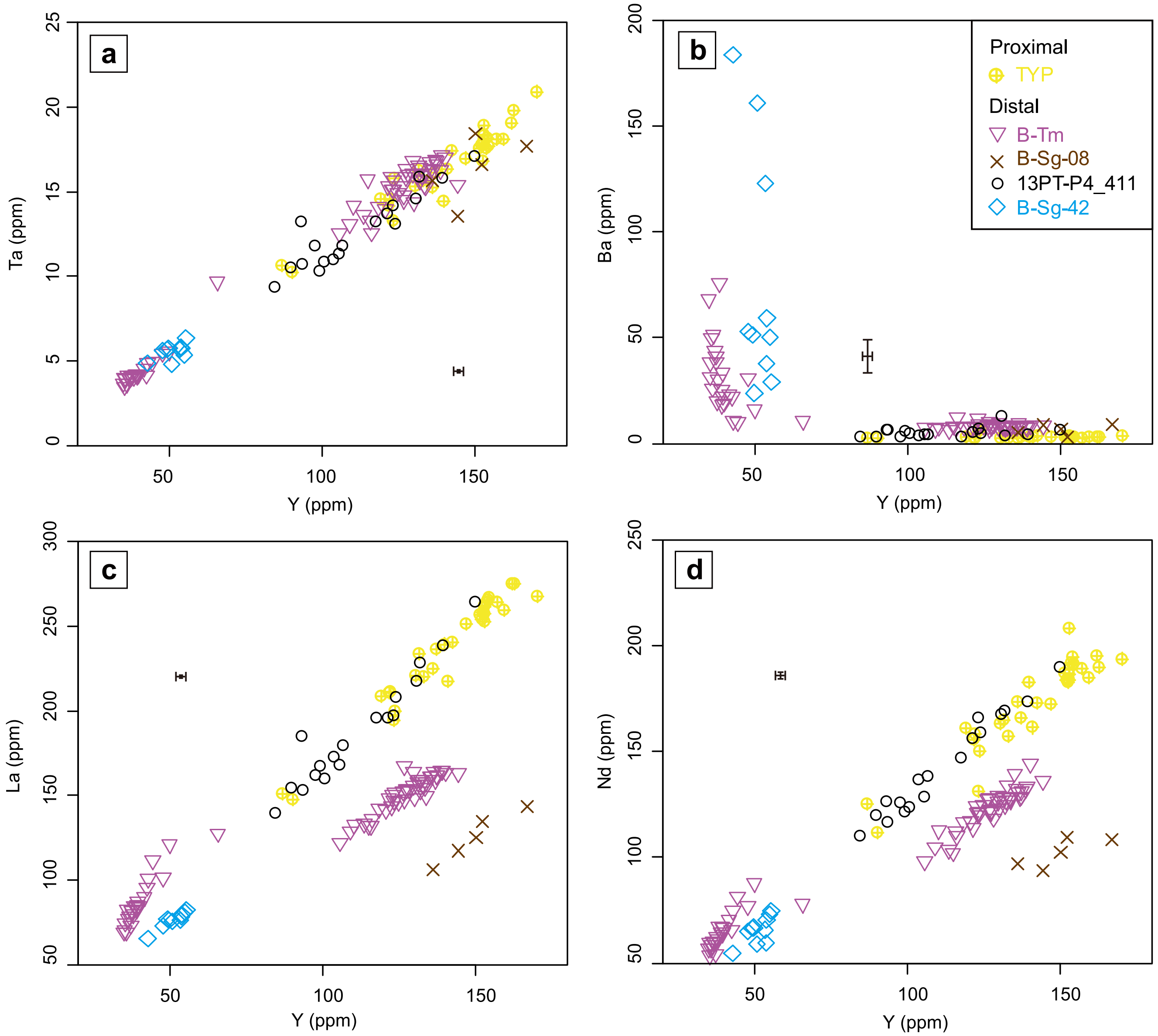

Figure 5. (a–d) Trace element bivariate plots showing glass compositions of the proximal Tianwen Yellow Pumice deposit (this study), distal 13PT-P4_411 tephra (this study), along with other distal Changbaishan tephras whose grain-specific trace element glass compositions are available. Detailed information and references of the distal Changbaishan tephras see Table 3. Error bars represent 2x standard deviation of repeat analyses of the ATHO-G standard glass. Reference data sources: B-Tm (Chen et al., 2016), B-Sg-08 and B-Sg-42 (McLean et al., 2020).

Among these nine distal eruption records (Table 3), glass compositions of the proximal TYP only match with those of the 13PT-P4_411 cryptotephra, and can be clearly distinguished from the other distal Changbaishan tephras at the major and minor element level (Figure 4). This geochemical consistency between the proximal TYP deposit and the distal 13PT-P4_411 cryptotephra is further underpinned by our reported grain-specific trace element data (Table 2). We find that trace element glass compositions of the two tephras are also consistent with each other (Figure 5), although analyses of the TYP glasses are more concentrated on the high Y end-member (e.g., Figure 5c) which could be due to bias on sampling of the very thick proximal deposit. Nevertheless, the compositional ranges and variations of glasses of the two tephra deposits are very similar in most of the analyzed trace elements (Table 2). Mantle-normalized spider diagram also confirms that the multi-element profiles of glasses of the two tephras have similar distribution pattern and enrichment level for incompatible elements (Figure 6). When compared to other Changbaishan tephras, the TYP and 13PT-P4_411 display similar glass

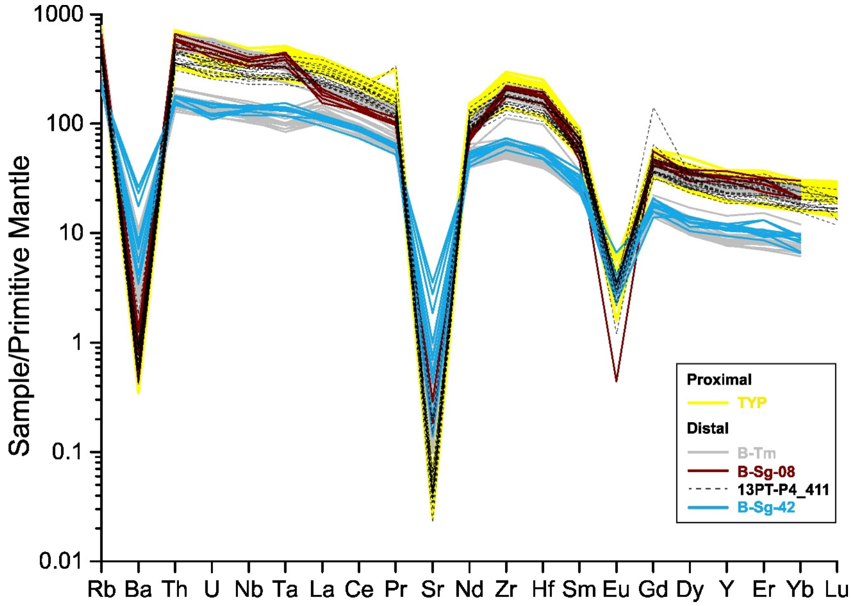

Figure 6. Primitive mantle normalized trace element compositions of glasses from the proximal Tianwen Yellow Pumice deposit (this study) and distal 13PT-P4_411 tephra (this study), along with other distal Changbaishan tephras for comparison. Reference data sources: B-Tm (Chen et al., 2016), B-Sg-08 and B-Sg-42 (McLean et al., 2020).

compositions with those of the B-Sg-08 and the high Y (more enriched) end-member of the B-Tm in some of the analyzed trace elements (e.g., Ta and Ba; Figures 5a and 5b). This similarity is also partially evident in their multi-element profiles (Figure 6). However, the TYP and 13PT-P4_411 glasses can be distinctly differentiated from other Changbaishan tephras (e.g., B-Tm, B-Sg-08, and B-Sg-42) using their significantly elevated light rare earth element (i.e., La, Ce, Pr, and Nd) concentrations (Figures 5c, 5d, and 6), which provide strong diagnostic evidence supporting that the two tephras originate from the same eruption.

In summary, the compositional affinity between the proximal TYP and the distal 13PT-P4_411 tephras at major, minor and trace element levels confirms that 13PT-P4_411 tephra originates from Changbaishan. More importantly, we show that glasses of the two tephra deposits are compositionally distinctive enough to be differentiated from all other Changbaishan tephras spanning the last ca. 100 ka (Figures 4–6). This unique geochemical signature allows an unambiguous proximal–distal tephra correlation between the TYP and 13PT-P4_411 (Figure 4d). Our finding questions the tephra correlation between the TYP and the ca. 51 ka B-J proposed by Pan et al. (2020), as glass compositions of the two tephras do not match at the major and minor element level (Figures 4a–4c; see Figure S2 in Supporting Information S1 for more details).

5.2. Precise Timing of TYP Eruption and Revised Eruption History of Changbaishan

Given the established proximal–distal tephra correlation, the TYP eruption can be dated to 29,921–29,255 cal yr BP (95.4%) utilizing age of the 13PT-P4_411 tephra. To further resolve the eruption timing, we have built a deposition model incorporating all available stratigraphic and chronological information of tephra layers identified in the 13PT-P4 record. The model includes six well-dated tephra layers (B-Tm, U-1, U-2, K-Ah, U-3, and U-Oki) that were previously identified in the Holocene core section (Chen et al., 2022). The presence of the AT tephra reported herein allows the use of its precise ^{14}C-verified varve age (29,627 yr BP, Mingram et al., 2018) from Lake Sihailongwan (SHL, Figure 1a) to constrain the marine deposition model. Along with the ^{14}C date of the 13PT-P4_411 tephra, a formal Bayesian deposition model has been constructed, which is based on a *P_Sequence* deposition model (Bronk Ramsey, 2008), incorporating a variable *k* parameter (Bronk Ramsey & Lee, 2013), a "General" *Outlier_Model* (Bronk Ramsey, 2009) and the latest IntCal20 calibration curve (Reimer et al., 2020). The 95.4% Highest Probability Density ranges for the deposition model are illustrated in Figure 7a. With the additional depositional and chronological constraints, the uncertainty of age of the 13PT-P4_411 tephra, and thus the TYP eruption, is narrowed to 29,948–29,625 cal yr BP (95.4%, Figure 7b).

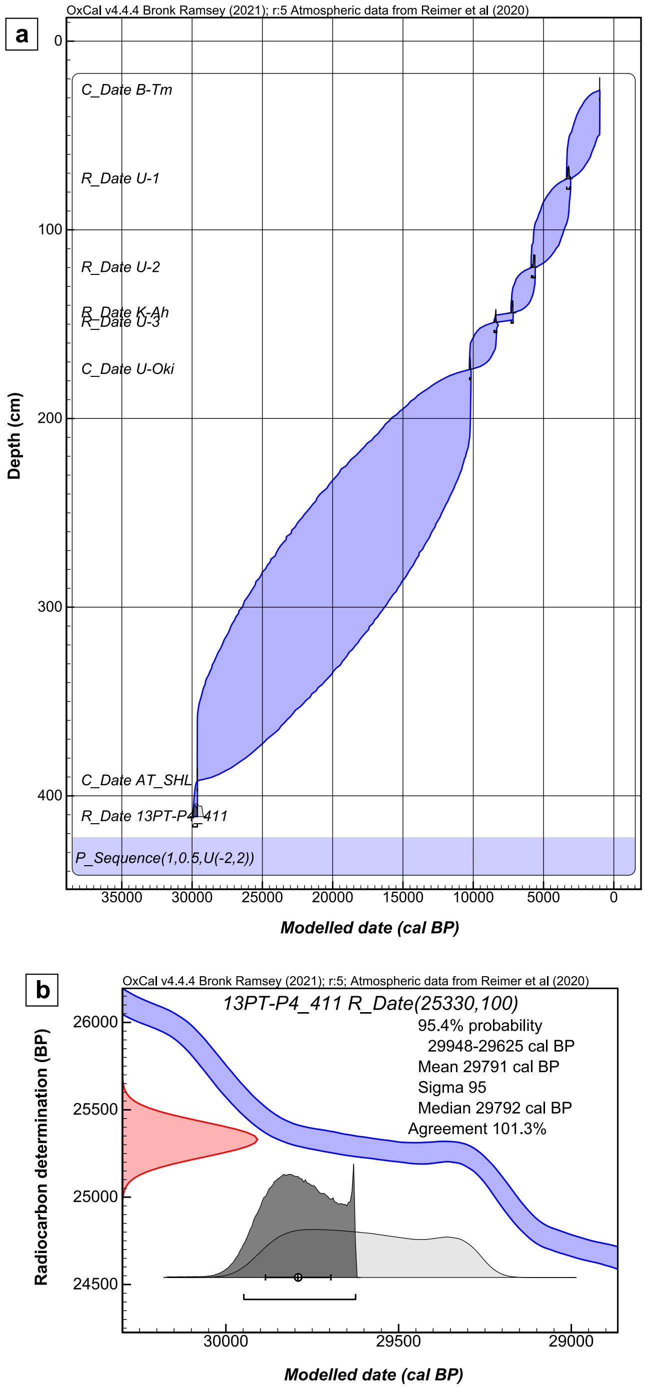

Figure 7. 95.4% Highest Probability Density ranges for (a) deposition model of the 13PT-P4 core for the last 30 ka core section and (b) 13PT-P4_411 tephra. The model utilizes chronological information of the six Holocene tephra layers identified in the core (Chen et al., 2022), the SHL Aira-Tanzawa tephra age (Mingram et al., 2018) and the ^{14}C date for the 13PT-P4_411 tephra (this study), along with their stratigraphic (depth) information. The model is constructed using Oxcal (v4.4.4; Bronk Ramsey, 2021), employing a *P_Sequence* deposition model (Bronk Ramsey, 2008) with a variable *k* parameter (Bronk Ramsey & Lee, 2013), a "General" *Outlier_Model* (Bronk Ramsey, 2009), and the IntCal20 calibration curve (Reimer et al., 2020).

In contrast to previous studies that have yielded a range of very different and contradictory ages for the TYP (Figure 1c), our age-depth model based on ^{14}C dates and tephrochronology provides a robust age for the eruption, thus improving the understanding of the eruption history of Changbaishan. In the proximal Tianwen Summit record three distinct eruptive episodes are now clearly identified and unambiguously dated (Figure 4d). These include the ca. 29.8 ka (this study) TYP eruption producing the yellow to gray lapilli fall deposit, the ca. 8–7 ka (Pan et al., 2020, 2022; Sun et al., 2018) Qixiangzhan clastogenic lava flow eruption and the 946 CE (Oppenheimer et al., 2017; Sigl et al., 2015; Xu et al., 2013) ME that produced light gray to black lapilli fall deposits (Chen et al., 2016). Evidence presented by Sun et al. (2017) and Yun et al. (2023) also shows that there might be several small-scale activities post-dating the ME, which require further verification. From a distal viewpoint, our discovery of the Changbaishan 13PT-P4_411 tephra discloses a previously unknown eruptive episode of the volcano, which in turn helps clarify the proximal tephrostratigraphy (Figure 4d). This finding complements our knowledge of explosive activities of Changbaishan and leads to a reevaluation of its magmatic resurgence. The volcano is now shown to have erupted violently at least nine times over the last 86 ka (Figure 4d, Table 3), resulting in an average return period of ca. 9.5 ka. It is noteworthy that the volcano has been particularly active during ca. 51–24 ka BP (Figure 4d), when the average return period was shortened to ca. 5 ka. Identification of the triggers for this increased activity warrants further investigation. Importantly, such evaluation would not be achievable if based only on studies of the frequently incomplete or patchy proximal outcrop sequences. Our results demonstrate the value of tephrostratigraphic approaches applied to distal deposits for reliable reconstruction of explosive volcanism of Changbaishan, which is essential for hazard risk assessment at this dangerous volcano.

5.3. Climatostratigraphical Context and Synchronization Potential of TYP Tephra

Widely dispersed tephra layers associated in time with important climatic events are considered to be valuable in testing leads and lags of abrupt changes in different climate systems (Lane et al., 2013; Reinig et al., 2021). Although the magnitude of the TYP eruption remains a matter of speculation, by identifying cryptotephra at a distance of ca. 600 km from the vent, we show, for the first time, that ash from the eruption was widely dispersed (Figure 1a). The high concentration of glass shards in the marine record (>10,000 shards/g of dry sediment) indicates tephra dispersion well beyond the 13PT-P4 site. In addition, our age determination (29,948–29,625 cal yr BP) shows that the TYP eruption is coeval with the phase of maximum cooling during the Greenland Stadial known as Heinrich Event 3 (H3, Bond et al., 1992; Figure 8a). South China speleothem isotope records (Cheng et al., 2016; Y. J. Wang et al., 2001) have shown that this hemispheric-scale climatic oscillation also impacted the Asian monsoon domain and led to decreased moisture levels (Figure 8b). A marked change in climatic conditions in the study region is also documented in the palynological record of Lake SHL (Mingram et al., 2018) located ca. 120 km west of Changbaishan (Figure 1a). A strong decrease in the proportion of tree and shrub (arboreal) pollen suggests colder and drier conditions around the lake at ca. 29.9–29.6 ka BP (Figure 8c). The coincidence of the TYP eruption with those regional to hemispheric-scale climatic changes (Figure 8) indicates significant potential of the associated tephra layer as a key marker in sediment-based palaeoenvironmental studies. Taken together with its wide

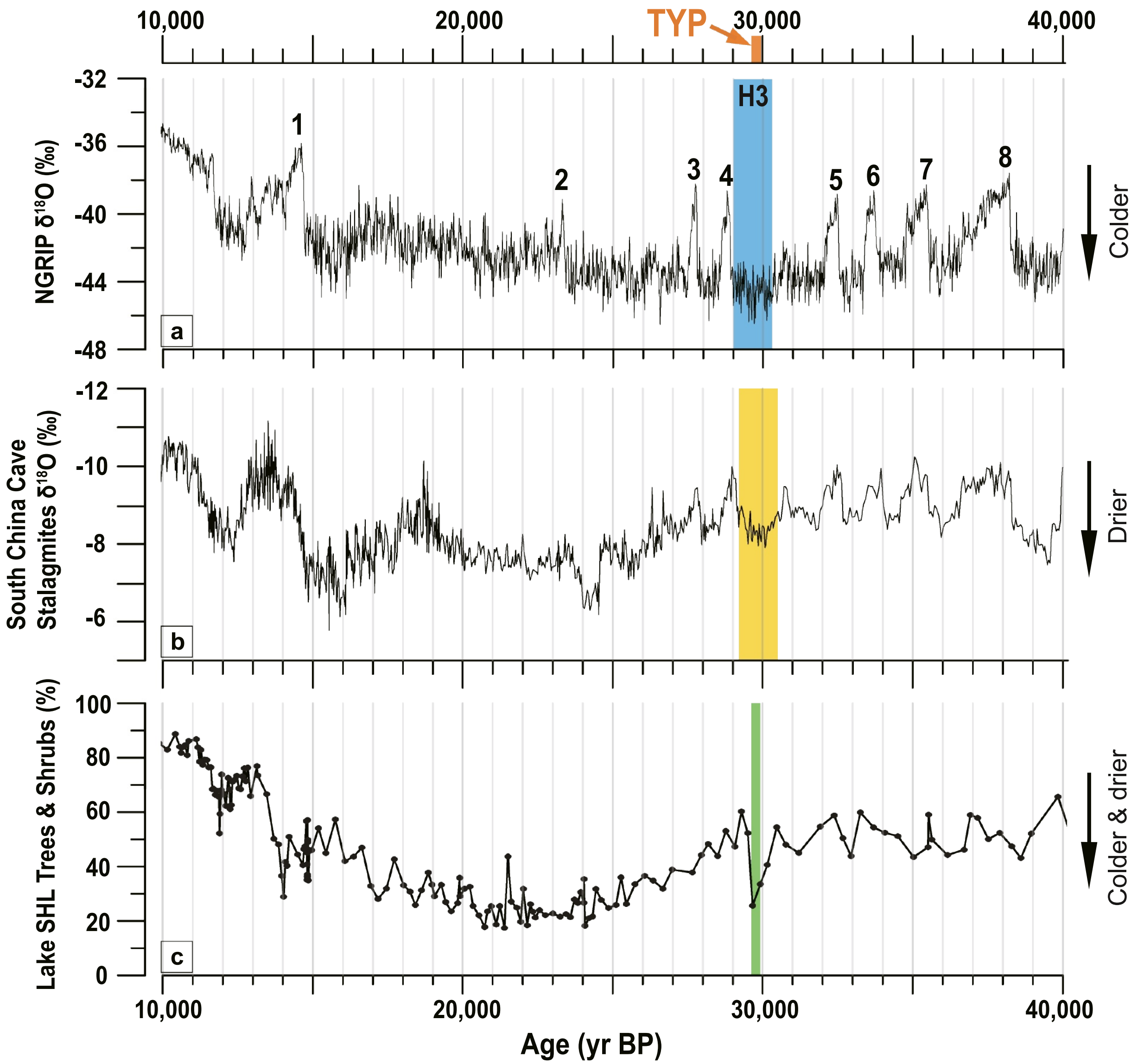

Figure 8. (a) Oxygen isotope record of Greenland ice core (North Greenland Ice Core Project et al., 2004), (b) oxygen isotope records of South China cave stalagmites (Cheng et al., 2016; Y. J. Wang et al., 2001), and (c) arboreal pollen record of Lake SHL (Mingram et al., 2018) for 40–10 ka BP. The stratigraphic position of the Tianwen Yellow Pumice tephra is shown using an orange vertical bar based on its age estimate from this study. The Heinrich Event 3 (Bond et al., 1992, 1993) is illustrated on the ice core and cave stalagmite records using vertical blue and yellow bars, respectively. A green vertical bar shows the period when climatic conditions in NE China experienced significant deterioration indicated by the arboreal pollen record of Lake SHL.

geographic distribution, the TYP tephra can therefore serve as an excellent climato- and chrono-stratigraphic marker for dating and synchronizing records of past climatic and environmental changes, and thus improve our ability to evaluate regional variability of the major climatic oscillation and its driving mechanism.

6. Conclusions

A cryptotephra layer (13PT-P4_411) has been identified in sediment core 13PT-P4 from the SW East Sea, intercalating tephra layers from the Ulleungdo (South Korea) and Aira (Japan) volcanoes. Grain-specific major, minor and trace element glass compositions reveal that the cryptotephra is sourced from Changbaishan (China/North Korea). Notably, among all documented distal Changbaishan tephras spanning the last 100 ka, the 13PT-P4_411 emerges as the sole candidate that can be geochemically correlated to the proximal TYP deposit of the volcano, thus suggesting a reliable tephra correlation for the TYP eruption.

An age-depth model incorporating tephrochronology, ^{14}C dating of marine sediment, and varve-chronology-based tephra age suggests an age of 29,948–29,625 cal yr BP (95.4%) for the 13PT-P4_411 tephra, and consequently the TYP eruption. The resulting robust new date resolves the long-standing controversy surrounding this major eruption and leads to a revision of the broader eruption history of Changbaishan. Altogether, nine explosive activities are recorded in distal sedimentary archives over the last ca. 100 ka, which show that the volcano has been particularly active during ca. 51–24 ka BP. In contrast, only three of these episodes (i.e., TYP, Qixiangzhan and ME) have thus far been clearly identified in the proximal outcrops, highlighting the necessity of employing a distal tephrostratigraphic approach to comprehend the eruption history of Changbaishan.

The identification of the TYP tephra ca. 600 km away from the volcano demonstrates, for the first time, significant dispersal potential of ash from the eruption. Moreover, the TYP eruption is synchronous with regional to hemispheric-scale climatic oscillation known as Heinrich Event 3 (H3), as palaeo-proxy records from Greenland and China demonstrate. The wide distribution and precise age determination of the TYP tephra make it a key climato- and chrono-stratigraphic marker for dating and synchronizing records of past climatic changes, and for evaluating leads and lags in environmental response to H3 in East Asia. Identification of the TYP tephra in high-resolution palaeoenvironmental archives becomes therefore a very important task for answering these questions.

Data Availability Statement

Data presented in this study (Chen et al., 2023) are included in Supporting Information S1 and are archived in the Figshare repository (https://doi.org/10.6084/m9.figshare.24844539).

Acknowledgments

This work was jointly supported by the National Natural Science Foundation of China (Grant 42102335), the PI Project of Southern Marine Science and Engineering Guangdong Laboratory (Guangzhou) (GML2022006), and the Early Career Research Program of the State Key Laboratory of Isotope Geochemistry. C. Leipe acknowledges financial support by the European Research Council Starting Grant 851102, Fruits of Eurasia: Domestication and Dispersal (FEDD). We thank the scientists, captains, and crews of the R/V *Tamhae II* during the KIGAM Expedition in 2013 (GP2012-027). We would also like to thank Prof. Martin Menzies for his assistance in the field, Dr. Chris Hayward for his help during EPMA sessions, Dr. Jian Yin for help with figure production, and Dr. Le Zhang for beneficial discussions. The authors would like to thank Prof. Shanaka de Silva and the anonymous reviewers for their constructive feedback on earlier versions of this manuscript, as well as Dr. Mark Dekkers for handing the manuscript. This is contribution No. IS-3497 from GIGCAS.

References

Albert, P. G., Smith, V. C., Suzuki, T., McLean, D., Tomlinson, E. L., Miyabuchi, Y., et al. (2019). Geochemical characterisation of the Late Quaternary widespread Japanese tephrostratigraphic markers and correlations to the Lake Suigetsu sedimentary archive (SG06 core). *Quaternary Geochronology*, *52*, 103–131. https://doi.org/10.1016/j.quageo.2019.01.005

Albert, P. G., Smith, V. C., Suzuki, T., Tomlinson, E. L., Nakagawa, T., McLean, D., et al. (2018). Constraints on the frequency and dispersal of explosive eruptions at Sambe and Daisen volcanoes (South-West Japan arc) from the distal Lake Suigetsu record (SG06 core). *Earth-Science Reviews*, *185*, 1004–1028. https://doi.org/10.1016/j.earscirev.2018.07.003

Alves, E. Q., Macario, K., Ascough, P., & Bronk Ramsey, C. (2018). The worldwide marine radiocarbon reservoir effect: Definitions, mechanisms, and prospects. *Reviews of Geophysics*, *56*(1), 278–305. https://doi.org/10.1002/2017rg000588

Blockley, S. P. E., Pyne-O'Donnell, S. D. F., Lowe, J. J., Matthews, I. P., Stone, A., Pollard, A. M., et al. (2005). A new and less destructive laboratory procedure for the physical separation of distal glass tephra shards from sediments. *Quaternary Science Reviews*, *24*(16–17), 1952–1960. https://doi.org/10.1016/j.quascirev.2004.12.008

Bond, G., Broecker, W., Johnsen, S., McManus, J., Labeyrie, L., Jouzel, J., & Bonani, G. (1993). Correlations between climate records from North Atlantic sediments and Greenland ice. *Nature*, *365*(6442), 143–147. https://doi.org/10.1038/365143a0

Bond, G., Heinrich, H., Broecker, W., Labeyrie, L., McManus, J., Andrews, J., et al. (1992). Evidence for massive discharges of icebergs into the North Atlantic Ocean during the last glacial period. *Nature*, *360*(6401), 245–249. https://doi.org/10.1038/360245a0

Bronk Ramsey, C. (2008). Deposition models for chronological records. *Quaternary Science Reviews*, *27*(1), 42–60. https://doi.org/10.1016/j.quascirev.2007.01.019

Bronk Ramsey, C. (2009). Dealing with outliers and offsets in radiocarbon dating. *Radiocarbon*, *51*(3), 1023–1045. https://doi.org/10.1017/s0033822200034093

Bronk Ramsey, C. (2021). OxCal 4.4.4. Retrieved from http://c14.arch.ox.ac.uk/oxcal

Bronk Ramsey, C., & Lee, S. (2013). Recent and planned developments of the program OxCal. *Radiocarbon*, *55*(2), 720–730. https://doi.org/10.2458/azu_js_rc.55.16215

Chen, X.-Y., Blockley, S. P. E., Fletcher, R., Zhang, S., Kim, J.-H., Park, M.-H., et al. (2022). Holocene tephrostratigraphy in the East Sea/Japan Sea: Implications for eruptive history of Ulleungdo volcano and potential for hemispheric synchronization of sedimentary archives. *Journal of Geophysical Research: Solid Earth*, *127*(2), e2021JB023243. https://doi.org/10.1029/2021jb023243

Chen, X.-Y., Blockley, S. P. E., Tarasov, P. E., Xu, Y.-G., McLean, D., Tomlinson, E. L., et al. (2016). Clarifying the distal to proximal tephrochronology of the Millennium (B–Tm) eruption, Changbaishan volcano, northeast China. *Quaternary Geochronology*, *33*, 61–75. https://doi.org/10.1016/j.quageo.2016.02.003

Chen, X.-Y., McLean, D., Blockley, S. P. E., Tarasov, P. E., Xu, Y.-G., & Menzies, M. A. (2019). Developing a Holocene tephrostratigraphy for northern Japan using the sedimentary record from Lake Kushu, Rebun Island. *Quaternary Science Reviews*, *215*, 272–292. https://doi.org/10.1016/j.quascirev.2019.05.017

Chen, X.-Y., Xu, Y.-G., Tarasov, P. E., Leipe, C., Kim, J.-H., Yan, S., et al. (2023). Revisiting the Tianwen Yellow Pumice (TYP) eruption of Changbaishan volcano: Tephra correlation, eruption timing and its climatostratigraphical context [Dataset]. *Figshare*. https://doi.org/10.6084/m9.figshare.24844539

Cheng, H., Edwards, R. L., Sinha, A., Spötl, C., Yi, L., Chen, S., et al. (2016). The Asian monsoon over the past 640,000 years and ice age terminations. *Nature*, *534*(7609), 640–646. https://doi.org/10.1038/nature18591

Chun, J.-H., Cheong, D., Lee, Y.-J., Kwon, Y.-I., & Kim, B.-C. (2006). Stratigraphic implications as a time marker of the B-J tephra erupted from Baegdusan volcano discovered in the marine cores of the East Sea/Japan Sea during the late Pleistocene. *Journal of the Geological Society of Korea*, *42*(1), 31–42.

Chun, J.-H., Han, S.-J., & Cheong, D.-K. (1997). Tephrostratigraphy in the Ulleung basin, East Sea: Late Pleistocene to Holocene. *Geosciences Journal*, *1*(3), 154–166. https://doi.org/10.1007/bf02910207

Derkachev, A. N., Utkin, I. V., Nikolaeva, N. A., Gorbarenko, S. A., Malakhova, G. I., Portnyagin, M. V., et al. (2019). Tephra layers of large explosive eruptions of Baitoushan/Changbaishan volcano in the Japan Sea sediments. *Quaternary International*, *519*, 200–214. https://doi.org/10.1016/j.quaint.2019.01.043

Guffanti, M., Mayberry, G. C., Casadevall, T. J., & Wunderman, R. (2009). Volcanic hazards to airports. *Natural Hazards*, *51*(2), 287–302. https://doi.org/10.1007/s11069-008-9254-2

Hayward, C. (2011). High spatial resolution electron probe microanalysis of tephras and melt inclusions without beam-induced chemical modification. *The Holocene*, *22*(1), 119–125. https://doi.org/10.1177/0959683611409777

Horn, S., & Schmincke, H.-U. (2000). Volatile emission during the eruption of Baitoushan volcano (China/North Korea) ca. 969 AD. *Bulletin of Volcanology*, *61*(8), 537–555. https://doi.org/10.1007/s004450050010

Iacovino, K., Ju-Song, K., Sisson, T., Lowenstern, J., Kuk-Hun, R., Jong-Nam, J., et al. (2016). Quantifying gas emissions from the "Millennium eruption" of Paektu volcano, democratic People's Republic of Korea/China. *Science Advances*, *2*(11), e1600913. https://doi.org/10.1126/sciadv.1600913

Ikeda, A., Okuno, M., Nakamura, T., Tsutsui, M., & Kobayashi, T. J. T. Q. R. (1995). Accelerator mass spectrometric ^{14}C dating of charred wood in the Osumi pumice fall and the Ito ignimbrite from Aira Caldera, Southern Kyushu, Japan. *The Quaternary Research (Daiyonki-Kenkyu)*, *34*(5), 377–379. https://doi.org/10.4116/jaqua.34.5_377

Ikehara, K., Kikkawa, K., & Chun, J.-H. (2004). Origin and correlation of three tephras that erupted during oxygen isotope stage 3 found in cores from the Yamato Basin, Central Japan Sea. *The Quaternary Research (Daiyonki-Kenkyu)*, *43*(3), 201–212. https://doi.org/10.4116/jaqua.43.201

Ji, F., Li, J., & Zheng, R. (1999). The preliminary study of TL chronology for recent eruptive materials in Changbaishan Tianchi volcano. *Geological Review*, *45*, 282–286.

Jochum, K. P., Stoll, B., Herwig, K., Willbold, M., Hofmann, A. W., Amini, M., et al. (2006). MPI-DING reference glasses for in situ microanalysis: New reference values for element concentrations and isotope ratios. *Geochemistry, Geophysics, Geosystems*, *7*(2), Q02008. https://doi.org/10.1029/2005GC001060

Lane, C. S., Brauer, A., Blockley, S. P. E., & Dulski, P. (2013). Volcanic ash reveals time-transgressive abrupt climate change during the Younger Dryas. *Geology*, *41*(12), 1251–1254. https://doi.org/10.1130/g34867.1

Le Bas, M. J., Le Maitre, R. W., Streckeisen, A., & Zanettin, B. (1986). A chemical classification of volcanic rocks based on the total alkali-silica diagram. *Journal of Petrology*, *27*(3), 745–750. https://doi.org/10.1093/petrology/27.3.745

Li, M., Peng, C., Wang, M., Yang, Y., Zhang, K., Li, P., et al. (2017). Spatial patterns of leaf $\delta^{13}C$ and its relationship with plant functional groups and environmental factors in China. *Journal of Geophysical Research: Biogeosciences*, *122*(7), 1564–1575. https://doi.org/10.1002/2016jg003529

Lim, C., Toyoda, K., Ikehara, K., & Peate, D. W. (2013). Late quaternary tephrostratigraphy of Baegdusan and Ulleung volcanoes using marine sediments in the Japan Sea/East Sea. *Quaternary Research*, *80*(1), 76–87. https://doi.org/10.1016/j.yqres.2013.04.002

Liu, R., Wei, H., & Li, J. (1998). *The latest eruptions from Tianchi volcano, Changbaishan*. SciencePress.

Lowe, D. J. (2011). Tephrochronology and its application: A review. *Quaternary Geochronology*, *6*(2), 107–153. https://doi.org/10.1016/j.quageo.2010.08.003

Machida, H., & Arai, F. (2003). *Atlas of tephra in and around Japan* (Revised ed.). University of Tokyo press.

McLean, D., Albert, P. G., Nakagawa, T., Staff, R. A., Suzuki, T., & Smith, V. C. (2016). Identification of the Changbaishan 'Millennium' (B-Tm) eruption deposit in the lake Suigetsu (SG06) sedimentary archive, Japan: Synchronisation of hemispheric-wide palaeoclimate archives. *Quaternary Science Reviews*, *150*, 301–307. https://doi.org/10.1016/j.quascirev.2016.08.022

McLean, D., Albert, P. G., Nakagawa, T., Suzuki, T., Staff, R. A., Yamada, K., et al. (2018). Integrating the Holocene tephrostratigraphy for East Asia using a high-resolution cryptotephra study from Lake Suigetsu (SG14 core), central Japan. *Quaternary Science Reviews*, *183*, 36–58. https://doi.org/10.1016/j.quascirev.2017.12.013

McLean, D., Albert, P. G., Suzuki, T., Nakagawa, T., Kimura, J.-I., Chang, Q., et al. (2020). Refining the eruptive history of Ulleungdo and Changbaishan volcanoes (East Asia) over the last 86 kyrs using distal sedimentary records. *Journal of Volcanology and Geothermal Research*, *389*, 106669. https://doi.org/10.1016/j.jvolgeores.2019.106669

Mingram, J., Stebich, M., Schettler, G., Hu, Y., Rioual, P., Nowaczyk, N., et al. (2018). Millennial-scale East Asian monsoon variability of the last glacial deduced from annually laminated sediments from lake Sihailongwan, NE China. *Quaternary Science Reviews*, *201*, 57–76. https://doi.org/10.1016/j.quascirev.2018.09.023

Muglia, J., Mulitza, S., Repschläger, J., Schmittner, A., Lembke-Jene, L., Lisiecki, L., et al. (2023). A global synthesis of high-resolution stable isotope data from benthic foraminifera of the last deglaciation. *Scientific Data*, *10*(1), 131. https://doi.org/10.1038/s41597-023-02024-2

Newhall, C., Self, S., & Robock, A. (2018). Anticipating future Volcanic Explosivity Index (VEI) 7 eruptions and their chilling impacts. *Geosphere*, *14*(2), 572–603. https://doi.org/10.1130/ges01513.1

North Greenland Ice Core Project, Andersen, K. K., Azuma, N., Barnola, J. M., Bigler, M., Biscaye, P., et al. (2004). High-resolution record of Northern Hemisphere climate extending into the last interglacial period. *Nature*, *431*(7005), 147–151. https://doi.org/10.1038/nature02805

Oppenheimer, C., Wacker, L., Xu, J., Galván, J. D., Stoffel, M., Guillet, S., et al. (2017). Multi-proxy dating the 'Millennium eruption' of Changbaishan to late 946 CE. *Quaternary Science Reviews*, *158*, 164–171. https://doi.org/10.1016/j.quascirev.2016.12.024

Pan, B., de Silva, S. L., Danišík, M., Schmitt, A. K., & Miggins, D. P. (2022). The Qixiangzhan eruption, Changbaishan-Tianchi volcano, China/DPRK: New age constraints and their implications. *Scientific Reports*, *12*(1), 22485. https://doi.org/10.1038/s41598-022-27038-5

Pan, B., de Silva, S. L., Xu, J., Liu, S., & Xu, D. (2020). Late Pleistocene to present day eruptive history of the Changbaishan-Tianchi volcano, China/DPRK: New field, geochronological and chemical constraints. *Journal of Volcanology and Geothermal Research*, *399*, 106870. https://doi.org/10.1016/j.jvolgeores.2020.106870

Park, M.-H., Kim, I.-S., & Shin, J.-B. (2003). Characteristics of the late quaternary tephra layers in the East/Japan Sea and their new occurrences in western Ulleung Basin sediments. *Marine Geology*, *202*(3–4), 135–142. https://doi.org/10.1016/s0025-3227(03)00287-1

Paton, C., Hellstrom, J., Paul, B., Woodhead, J., & Hergt, J. (2011). Iolite: Freeware for the visualisation and processing of mass spectrometric data. *Journal of Analytical Atomic Spectrometry*, *26*(12), 2508–2518. https://doi.org/10.1039/c1ja10172b

Ramos, F. C., Heizler, M., Buettner, J., Gill, J., Wei, H., Dimond, C., & Scott, S. (2016). U-series and $^{40}Ar/^{39}Ar$ ages of Holocene volcanic rocks at Changbaishan volcano, China. *Geology*, *44*(7), 511–514. https://doi.org/10.1130/g37837.1

Reimer, P. J., Austin, W. E. N., Bard, E., Bayliss, A., Blackwell, P. G., Bronk Ramsey, C., et al. (2020). The IntCal20 Northern Hemisphere radiocarbon age calibration curve (0–55 cal kBP). *Radiocarbon*, *62*(4), 725–757. https://doi.org/10.1017/rdc.2020.41

Reimer, P. J., Baillie, M. G. L., Bard, E., Bayliss, A., Beck, J. W., Blackwell, P. G., et al. (2009). IntCal09 and Marine09 radiocarbon age calibration curves, 0–50,000 years cal BP. *Radiocarbon*, *51*(4), 1111–1150. https://doi.org/10.1017/s0033822200034202

Reinig, F., Wacker, L., Jöris, O., Oppenheimer, C., Guidobaldi, G., Nievergelt, D., et al. (2021). Precise date for the Laacher see eruption synchronizes the Younger Dryas. *Nature*, *595*(7865), 66–69. https://doi.org/10.1038/s41586-021-03608-x

Robock, A. (2000). Volcanic eruptions and climate. *Reviews of Geophysics*, *38*(2), 191–219. https://doi.org/10.1029/1998rg000054

Sigl, M., Winstrup, M., McConnell, J. R., Welten, K. C., Plunkett, G., Ludlow, F., et al. (2015). Timing and climate forcing of volcanic eruptions for the past 2,500 years. *Nature*, *523*(7562), 543–549. https://doi.org/10.1038/nature14565

Smith, V. C., Mark, D. F., Staff, R. A., Blockley, S. P. E., Ramsey, C. B., Bryant, C. L., et al. (2011). Toward establishing precise $^{40}Ar/^{39}Ar$ chronologies for late Pleistocene palaeoclimate archives: An example from the lake Suigetsu (Japan) sedimentary record. *Quaternary Science Reviews*, *30*(21–22), 2845–2850. https://doi.org/10.1016/j.quascirev.2011.06.020

Smith, V. C., Staff, R. A., Blockley, S. P. E., Bronk Ramsey, C., Nakagawa, T., Mark, D. F., et al. (2013). Identification and correlation of visible tephras in the lake Suigetsu SG06 sedimentary archive, Japan: Chronostratigraphic markers for synchronising of east Asian/west Pacific palaeoclimatic records across the last 150 ka. *Quaternary Science Reviews*, *67*(0), 121–137. https://doi.org/10.1016/j.quascirev.2013.01.026

Stockmarr, J. (1971). Tablets with spores used in absolute pollen analysis. *Pollen et Spores*, *13*, 615–621.

Stuiver, M., Pearson, G. W., & Braziunas, T. (1986). Radiocarbon age calibration of marine samples back to 9000 cal yr BP. *Radiocarbon*, *28*(2B), 980–1021. https://doi.org/10.1017/s0033822200060264

Sun, C., Liu, J., You, H., & Nemeth, K. (2017). Tephrostratigraphy of Changbaishan volcano, northeast China, since the mid-Holocene. *Quaternary Science Reviews*, *177*, 104–119. https://doi.org/10.1016/j.quascirev.2017.10.021

Sun, C., Plunkett, G., Liu, J., Zhao, H., Sigl, M., McConnell, J. R., et al. (2014). Ash from Changbaishan Millennium eruption recorded in Greenland ice: Implications for determining the eruption's timing and impact. *Geophysical Research Letters*, *41*(2), 694–701. https://doi.org/10.1002/2013gl058642

Sun, C., Wang, L., Plunkett, G., You, H., Zhu, Z., Zhang, L., et al. (2018). Ash from the Changbaishan Qixiangzhan eruption: A new early Holocene marker horizon across East Asia. *Journal of Geophysical Research: Solid Earth*, *123*(8), 6442–6450. https://doi.org/10.1029/2018jb015983

Sun, C., You, H., He, H., Zhang, L., Gao, J., Guo, W., et al. (2015). New evidence for the presence of Changbaishan Millennium eruption ash in the Longgang volcanic field, Northeast China. *Gondwana Research*, *28*(1), 52–60. https://doi.org/10.1016/j.gr.2015.01.013

Tomlinson, E. L., Arienzo, I., Civetta, L., Wulf, S., Smith, V. C., Hardiman, M., et al. (2012). Geochemistry of the Phlegraean fields (Italy) proximal sources for major Mediterranean tephras: Implications for the dispersal of Plinian and co-ignimbritic components of explosive eruptions. *Geochimica et Cosmochimica Acta*, *93*(0), 102–128. https://doi.org/10.1016/j.gca.2012.05.043

Tomlinson, E. L., Smith, V. C., Albert, P. G., Aydar, E., Civetta, L., Cioni, R., et al. (2015). The major and trace element glass compositions of the productive Mediterranean volcanic sources: Tools for correlating distal tephra layers in and around Europe. *Quaternary Science Reviews*, *118*, 48–66. https://doi.org/10.1016/j.quascirev.2014.10.028

Wang, F., Chen, W.-J., Peng, Z.-C., & Li, Q. (2001). Activity of Cangbaishan Tianchi volcano since late Pleistocene: The constrain from geochronology of high precision U-series TIMS method. *Geochimica*, *30*(1), 88–94.

Wang, Y. J., Cheng, H., Edwards, R. L., An, Z. S., Wu, J. Y., Shen, C.-C., & Dorale, J. A. (2001). A high-resolution absolute-dated late Pleistocene monsoon record from Hulu Cave, China. *Science*, *294*(5550), 2345–2348. https://doi.org/10.1126/science.1064618

Wei, H., Liu, G., & Gill, J. (2013). Review of eruptive activity at Tianchi volcano, Changbaishan, Northeast China: Implications for possible future eruptions. *Bulletin of Volcanology*, *75*(4), 1–14. https://doi.org/10.1007/s00445-013-0706-5

Xu, J., Liu, G., Wu, J., Ming, Y., Wang, Q., Cui, D., et al. (2012). Recent unrest of Changbaishan volcano, Northeast China: A precursor of a future eruption? *Geophysical Research Letters*, *39*(16), L16305. https://doi.org/10.1029/2012GL052600

Xu, J., Pan, B., Liu, T., Hajdas, I., Zhao, B., Yu, H., et al. (2013). Climatic impact of the Millennium eruption of Changbaishan volcano in China: New insights from high-precision radiocarbon wiggle-match dating. *Geophysical Research Letters*, *40*(1), 54–59. https://doi.org/10.1029/2012gl054246

Yang, L., Wang, F., Feng, H., Wu, L., & Shi, W. (2014). $^{40}Ar/^{39}Ar$ geochronology of Holocene volcanic activity at Changbaishan Tianchi volcano, Northeast China. *Quaternary Geochronology*, *21*, 106–114. https://doi.org/10.1016/j.quageo.2013.10.008

Yang, Q., Jenkins, S. F., Lerner, G. A., Li, W., Suzuki, T., McLean, D., et al. (2021). The Millennium eruption of Changbaishan Tianchi volcano is VEI 6, not 7. *Bulletin of Volcanology*, *83*(11), 74. https://doi.org/10.1007/s00445-021-01487-8

Yun, S.-H., Lee, J., Chang, C., & Oppenheimer, C. (2023). A re-assessment of historical records pertaining to the activity of Mt. Baekdu (Paektu, Tianchi) volcano. *Geoscience Letters*, *10*(1), 30. https://doi.org/10.1186/s40562-023-00286-7

Zhang, M., Guo, Z., Liu, J., Liu, G., Zhang, L., Lei, M., et al. (2018). The intraplate Changbaishan volcanic field (China/North Korea): A review on eruptive history, magma genesis, geodynamic significance, recent dynamics and potential hazards. *Earth-Science Reviews*, *187*, 19–52. https://doi.org/10.1016/j.earscirev.2018.07.011

References From the Supporting Information

Aoki, K. (2008). Revised age and distribution of ca. 87 ka Aso-4 tephra based on new evidence from the northwest Pacific Ocean. *Quaternary International*, *178*(1), 100–118. https://doi.org/10.1016/j.quaint.2007.02.005

Aoki, K., Irino, T., & Oba, T. (2008). Late Pleistocene tephrostratigraphy of the sediment core MD01-2421 collected off the Kashima coast, Japan. *The Quaternary Research (Daiyonki-kenkyu)*, *47*(6), 391–407. https://doi.org/10.4116/jaqua.47.391

Ito, H. (2014). Zircon U–Th–Pb dating using LA-ICP-MS: Simultaneous U–Pb and U–Th dating on the 0.1Ma Toya Tephra, Japan. *Journal of Volcanology and Geothermal Research*, *289*, 210–223. https://doi.org/10.1016/j.jvolgeores.2014.11.002

Miyairi, Y., Yoshida, K., Miyazaki, Y., Matsuzaki, H., & Kaneoka, I. (2004). Improved ^{14}C dating of a tephra layer (AT tephra, Japan) using AMS on selected organic fractions. *Nuclear Instruments and Methods in Physics Research Section B: Beam Interactions with Materials and Atoms*, *223–224*, 555–559. https://doi.org/10.1016/s0168-583x(04)00628-7

Okuno, M., Shiihara, M., Torii, M., Nakamura, T., Kim, K. H., Domitsu, H., et al. (2010). AMS radiocarbon dating of Holocene tephra layers on Ulleung Island, South Korea. *Radiocarbon*, *52*(3), 1465–1470. https://doi.org/10.1017/s0033822200046555

Uesawa, S., Nakagawa, M., & Umetsu, A. (2016). Explosive eruptive activity and temporal magmatic changes at Yotei Volcano during the last 50,000 years, southwest Hokkaido, Japan. *Journal of Volcanology and Geothermal Research*, *325*, 27–44. https://doi.org/10.1016/j.jvolgeores.2016.06.008